ELSEVIER

Journal of Photochemistry and Photobiology A: Chemistry 126 (1999) 99–109

Journal of Photochemistry and Photobiology A:Chemistry

www.elsevier.nl/locate/jphotochem

Efficient low temperature charge transfer in a self-assembled porphyrin aggregate

A. Willert [b], S. Bachilo [a], U. Rempel [b,*], A. Shulga [a], E. Zenkevich [a], C. von Borczyskowski [b]

[a] *Institute of Molecular and Atomic Physics, Academy of Sciences of Belarus, 70 F. Skaryna Avenue, Minsk 220072, Belarus*

[b] *Institut für Physik, Technische Universität Chemnitz, 09107 Chemnitz, Germany*

Accepted 12 May 1999

Abstract

Self-assembled triadic aggregates of porphyrins were formed from a covalently linked zinc-octaethyl-porphyrin dimer (ZnPD) and either of two different dipyridyl-substituted free base porphyrins, making use of the extra-ligation of zinc-porphyrin by the pyridyl-substituents of the free base porphyrins. The two free base porphyrins differ in the phenyl-substituents which are linked to them apart from the two pyridyl-groups. In one case these phenyl-substituents are pentafluorinated (H_2PF) while in the other case (H_2P) they are not. In the aggregate formed with H_2PF fluorescence quenching of both parts, ZnPD as well as H_2PF, indicates electron transfer from ZnPD to H_2PF which is effective down to 120 K. In the aggregate formed with H_2P the amount of population of the excited state H_2P is dependent on the solvent dielectric constant as well as on temperature. This is attributed to a close lying charge separated state which exchanges rapidly with the excited state of H_2P.

Keywords: Porphyrins; Electron transfer; Self-assembly; Time-resolved absorption

1. Introduction

Supramolecular porphyrin arrays have been used quite intensively in order to model energy and charge transfer processes in biological systems [1–6] or to gain insight into the principal possibilities of molecular electronics [7]. Apart from covalently linking the desired supramolecular subunits the strategy of self-assembly, using different kinds of non-covalent linkage of the subunits, has attracted a lot of interest [8–13]. We already demonstrated the feasibility of using the complexation of metallo-porphyrins by molecules with lone pair electrons (such as for example pyridine, chinuclidine or diazobicyclooctane) to form triadic [14] or even pentadic [15] porphyrin arrays. These systems are formed from zinc-porphyrin dimers and pyridyl-substituted free base porphyrins. The coordination of the nitrogen atoms of two of the pyridyl substituents as axial extra-ligands to the zinc-ions of the zinc-porphyrin dimer gives rise to complexation constants of the order of 10^6 to 10^7 M^{-1}. In the present work we compare two triadic complexes formed in this way, using steady-state and time-resolved optical spectroscopy. They consist of a 1,4-phenyl bridged zinc-octaethyl-porphyrin dimer (ZnPD), to which either of two dipyridyl-substituted free base porphyrins is attached. In case of 5,10-di(pentafluorophenyl)-15,20-dipyridyl free base porphyrin (H_2PF) both fluorescence from the ZnPD as well as from the H_2PF moiety are almost completely quenched, which is attributed to electron transfer resulting in a charge separated state which is considerably lower in energy as compared to the H_2PF locally excited S_1 state. This charge separated state becomes higher in energy when a 5,10-diphenyl-15,20-dipyridyl free base porphyrin (H_2P) is used to form the aggregate. Our results from steady-state and time-resolved optical spectroscopy indicate that in this case it is close to the excited H_2P state leading to an equilibrium population distribution among those states.

2. Experimental

The zinc-porphyrin dimer, 1,4-bis {[zinc(II)] 5-(2,3,7,8, 12,13,17,18-octaethylporphyrinyl)}benzene was synthesized and identified as described in our earlier paper [14]. 5,10-Bis(4-iso-propylphenyl)-15,20-bis (3-pyridyl)porphyrin was obtained by a cross-condensation [16] of 3-pyridinecarboxaldehyde 4.28 g (40 mmol) and 4-iso-propylbenzaldehyde

* Corresponding author. Fax +49-371-531-3060

1010-6030/99/$ – see front matter
PII: S1010-6030(99)00103-3

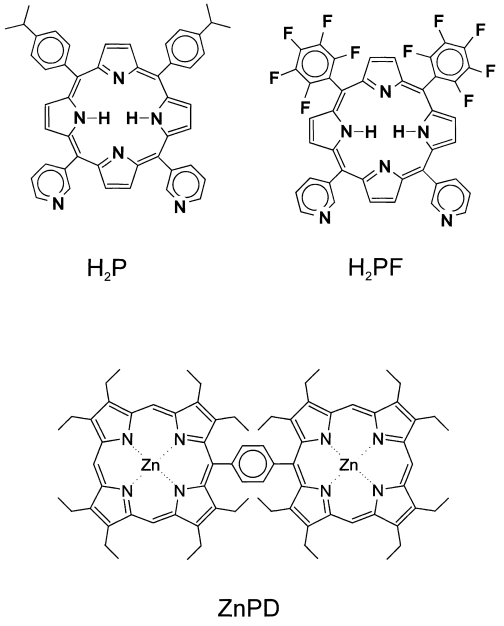

Fig. 1. Structures of the molecules used to form self-assembled aggregates: 5,10-diphenyl-15,20-dipyridyl free base porphyrin (H_2P), 5,10-di(pentafluorophenyl)-15,20-dipyridyl free base porphyrin (H_2PF) and 1,4 di(zinc-octaethylporphyrin) benzene (ZnPD).

5.92 g (40 mmol) with pyrrole 5.36 g (80 mmol) in boiling propionic acid (200 ml). After the evaporation of the solvent in vacuum the proper product (0.33 g) was separated by column chromatography. A chloroform diethyl-ether mixture (10 : 1) was applied as an eluent. The mixtures of chlorins were oxidized by 2,3-dichloro-5,6-dicyano-1,4-benzoquinone (DDQ) [17]. 5,10-Bis(penta-fluorophenyl)-15,20-bis(3-pyridyl)porphyrin (0.147 g) was obtained by the same procedure using 2.14 g (20 mmol) of 3-pyridinecarboxaldehyde, 3.92 g (20 mmol) of pentafluorophenylbenzaldehyde, 2.68 g (40 mmol) of pyrrole in 100 ml of propionic acid. In this case it was impossible to oxidize the admixtures of chlorins by DDQ. Therefore the pure porphyrin was separated from the middle part of zone upon the chromatography on a silica gel column (Merck, 230–400 mesh) using a benzene–chloroform–diethyl-ether mixture (60 : 30 : 2) as an eluent. In Fig. 1 the structures of the molecules are presented. To prepare the self-aggregated assemblies for steady-state spectroscopy ZnPD was dissolved in toluene (Aldrich HPLC grade) to a concentration of approximately 2×10^{-6} M in a 10 mm × 10 mm sample cell. The titration was performed by adding small quantities of a higher concentrated ($\approx 1 \times 10^{-4}$ M) toluene solution of the free base porphyrin, until the desired molar ratio of dimer and free-base was obtained. This process was monitored at each titration step by absorption and fluorescence spectroscopy. For pump-probe measurements much higher concentrated solutions were needed (5×10^{-5} M). No titration was performed in this case but both solutions were prepared to approximately this concentration and the necessary volumes from them were added according to the desired ratio (usually 1 : 1). As compared to our previous studies [14,15] toluene was used instead of methylcyclohexane because it provides better solubility for all of the molecules involved. No additional polar solvent component (CH_2Cl_2) is therefore necessary to predissolve the components. Steady-state spectra obtained in methylcyclohexane and toluene respectively do not show any significant differences. Air saturated samples were used in all cases. The steady-state fluorescence and excitation spectra were recorded on a Shimadzu RF-5001PC spectrofluorometer and absorption spectra on a Shimadzu UV-3101PC spectrophotometer. For temperature dependent measurements a homemade liquid nitrogen cryostat was used.

The laser source for the pump and probe measurements consists of a mode-locked titanium-sapphire laser (Coherent Mira Model 900B) pumped by a multiline Ar^+ laser (Coherent Innova 310, P_{cw}=8 W) and a Ti : sapphire regenerative amplifier system (Quantronix 4800 fs-3 K). The amplified laser pulses at 800 nm have an energy of 0.8 mJ at a repetition rate of 1 kHz. They are split into two parts. One part (30%) is used to generate a white-light continuum for the probe pulses by focusing it into a rotating quartz-plate. The other part (70%) is fed into an optical parametric amplifier (OPA) (Light conversion Ltd., TOPAS) to generate pump pulses tunable in wavelength from 480–750 nm or for frequency doubling to obtain 400 nm. The output from the OPA passes a 10.5 cm variable delay line (leading to a relative delay between pump and probe pulses of $-50 \ldots +650$ ps) before being focused into the sample cell by a 20 cm lens. The sample is placed in a spinning cell with 2 mm pathlength and 50 mm diameter. The spinning frequency was chosen to have a fresh excitation volume for each pump pulse (i.e. every 1 ms). To obtain the magic angle of 54.7° between pump and probe beam the polarization of the pump is rotated by a Soleil–Babinet compensator to the desired direction. The white light beam is split into equivalent probe and reference beams which are focused into the sample cell by a 14 cm lens. While the probe beam overlaps in the sample cell with the pump beam, the reference beam passes the sample 3 mm below the excitation area. Both beams are focused onto the entrance slit of a monochromator (SPEX 270M) and detected at the exit of it by two photodiodes separately. The signals are amplified and digitized at 1 kHz repetition rate. From the intensity of probe and reference beam the change in optical density is calculated by carefully taking stray light effects into account.

3. Results

3.1. Steady-state spectra

3.1.1. Formation of complexes

Upon titration of ZnPD with H_2PF the absorption bands of ZnPD clearly red-shift from 543 and 577 nm to 549 and 582 nm, which is typical of ZnPD complexation by

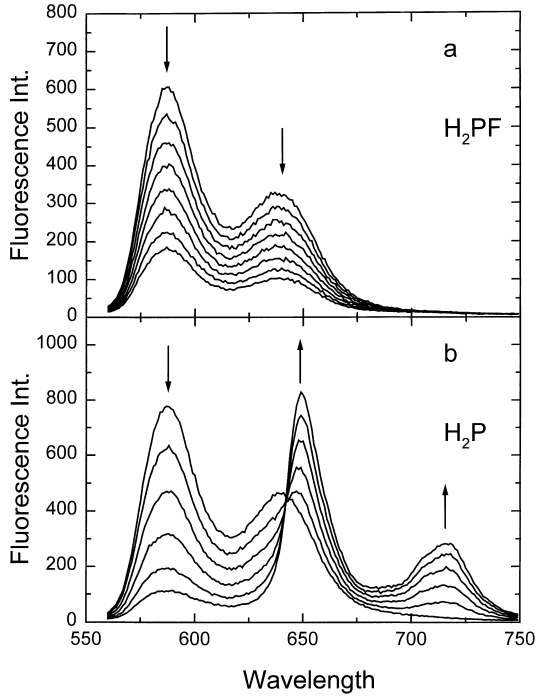

Fig. 2. (a) Fluorescence spectra (λ_{ex} = 546 nm) of ZnPD with different amounts of H_2PF. (Concentration of ZnPD at the beginning of titration ($c_{D,0}$) was 1.8×10^{-6} M^{-1}). Molar ratios x of H_2PF and ZnPD are 0.00, 0.13, 0.26, 0.40, 0.53, 0.66, 0.80 and 0.93. (b) Fluorescence spectra (λ_{ex} = 546 nm) of ZnPD with different amounts of H_2P. ($c_{D,0} = 2.2 \times 10^{-6}$ M^{-1}). Molar ratios x of H_2P and ZnPD are 0.0, 0.2, 0.4, 06, 0.8 and 1.0.

pyridine [18]. These spectra are very similar to those already described for a variety of triads formed from zinc porphyrin dimers and free base porphyrins [14]. The ground-state absorption spectra of the triads are practically solvent-independent and present themselves essentially as a superposition of the corresponding spectra of individual ZnPD and free base porphyrin extra-ligands. This indicates that the ground-state interactions between the two parts of triads are weak and the corresponding triad spectra do not represent a charge-transfer absorption.

While the absorption spectra of the titration experiment of ZnPD with H_2P or H_2PF are very similar, great differences are observed in fluorescence spectra. Those are compared in Fig. 2 where excitation was at 546 nm which is the isosbestic point for ZnPD complexation with pyridine. In both cases, as the aggregates are formed, quenching of ZnPD fluorescence (with its bands at 589 and 639 nm) is observed. While for the non-fluorinated triad H_2P fluorescence (with bands at 650 and 716 nm) increases with increasing concentration of extra ligand, in case of the fluorinated triad no H_2PF fluorescence is observed. Before looking at this difference in free base porphyrin fluorescence in more detail we would like to note that no red-shifted fluorescence bands typical of pyridine complexed ZnPD are detected in both cases. It thus is deduced that fluorescence observed at $\lambda < 610$ nm is completely due to ZnPD not bound in aggregates. Therefore the relative concentration of these non-bound dimers was calculated from the integrated fluorescence intensity between 570 and 610 nm. From the dependence of this concentration upon the added amount of free base porphyrin the complexation constant K_C was calculated to be 6×10^6 M^{-1} in case of the fluorinated triad and 2×10^7 M^{-1} in case of the non-fluorinated triad (error is up to 50% in both cases, which is the result of very high sensitivity of the calculation to small errors in concentration determination, which are assumed to be 5%).

Although the emission of the fluorinated extra-ligand is not visible in the fluorescence spectra in Fig. 2 a fluorescence excitation spectrum (monitored at 717 nm where the major part of fluorescence is from the extra-ligand) can still be observed (with appropriate signal amplification). It is presented in Fig. 3 together with those of H_2PF and of the non-fluorinated triad. In case of the non-fluorinated triad the fluorescence excitation spectrum obviously consists of bands corresponding to H_2P absorption (at 515 and 647 nm) as well as of bands corresponding to ZnPD absorption (at 551 and 586 nm). The fluorinated triad shows completely different behavior. The excitation spectrum in this case is identical in shape to that of the pure H_2PF (but much smaller), indicating, that no fluorescence is sensitized via ZnPD absorption. (It can be attributed completely to non-bound H_2PF.)

Even in the case of the non-fluorinated triad the H_2P fluorescence quantum efficiency is reduced as compared to the pure H_2P, when excited at 650 nm (where only H_2P absorbs) (Fig. 4 inset). To test whether charge transfer processes may be involved in this quenching which are expected to depend on the dielectric constant of the solvent, acetone was added to the previously pure toluene solution of the non-fluorinated triad. As shown in Fig. 4 this leads to a reduction of the free base fluorescence (bands at 650 and 714 nm) at both excitation wavelength of 650 nm (H_2P absorption) and 546 nm (ZnPD absorption). At excitation wavelength of 546 nm (i.e. into the ZnPD absorption band) at 0 and 3 vol% of acetone the H_2P fluorescence intensity is larger than that of the pure extra-ligand under the same conditions of excitation which indicates energy transfer from the excited ZnPD. (The fluorescence of the pure H_2P solution does not show fluorescence quenching upon acetone addition.) The intensity of the ZnPD fluorescence band at 590 nm (λ_{ex} = 546 nm) changes only slightly indicating that the triads are not destroyed upon acetone addition (from 17 to 22% of the intensity observed in pure ZnPD solution; i.e. the amount of non-bound dimers is changing accordingly). Fig. 5 reveals that the quenching of H_2P fluorescence intensity upon increasing polarity goes along with a change in excitation spectrum from 'triad-like' (i.e. bands corresponding to the absorption bands of H_2P and ZnPD) to 'H_2P-like'. Upon addition of 17 vol% of acetone the excitation spectrum is almost identical in shape to that of the extra ligand (H_2P).

Fluorescence spectra at different temperatures were taken for both kinds of triads. For the non-fluorinated triad such spectra in toluene and 7 vol% of acetone are shown in Fig.

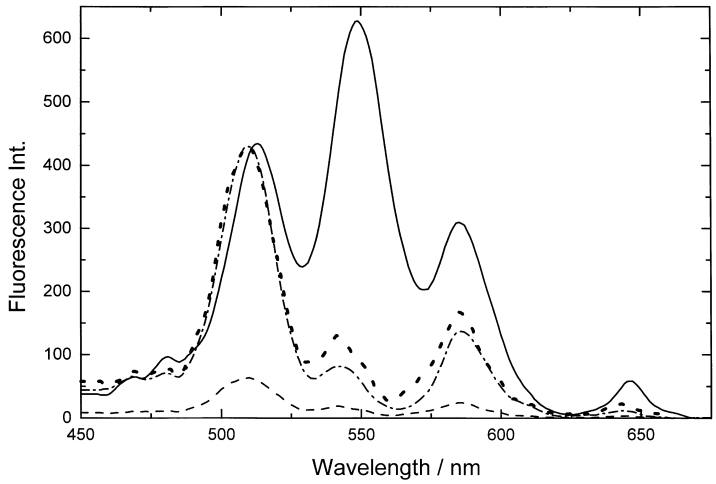

Fig. 3. Fluorescence excitation spectra (λ_{ex} = 714 nm) of non-fluorinated triad (————), fluorinated triad (— — —) and pure H_2PF (· – · – · –). Spectrum of the fluorinated triad multiplied by 6.82 (- - - - -).

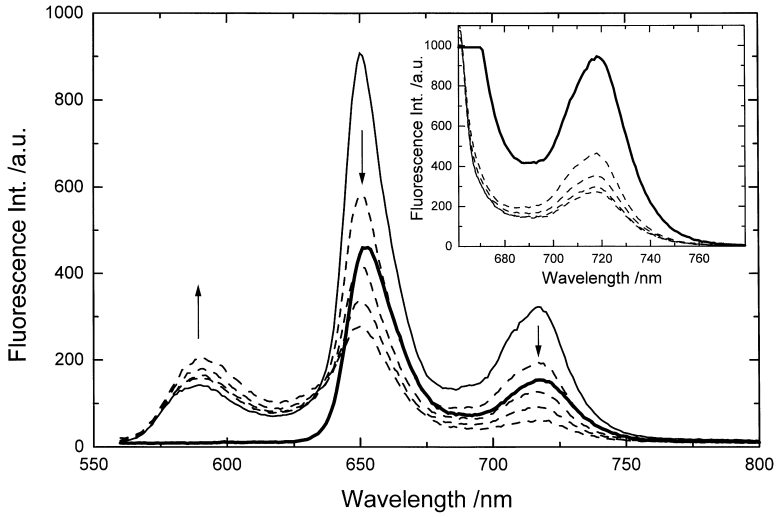

Fig. 4. Fluorescence spectra (λ_{ex} = 546 nm) of non-fluorinated triad (x = 0.92, $c_{D,0} = 2.6 \times 10^{-6}$ M) in toluene plus 0 (thin solid line), 3, 6, 9, 17 vol% of acetone (thin dashed lines, intensity decreases with increasing amount of acetone). H_2P in toluene at same concentration as in triad (bold line). Inset: as before but λ_{ex} = 650 nm.

6(b). At temperatures higher than 278 K an increase in ZnPD fluorescence indicates decomposition of the aggregates. At temperatures below 278 K the ZnPD fluorescence intensity remains constant but the fluorescence intensity of H_2P is decreased. Within experimental error no such reduction in H_2P fluorescence is observed in pure toluene solution.

Fluorescence spectra of the fluorinated triad at reduced temperature are shown in Fig. 6(a). The excitation wavelength was 545 nm, where the main part of absorption is due to the ZnPd moiety. From room temperature down to 164 K only fluorescence from the non-complexed ZnPD and no sensitized H_2PF fluorescence is observed. From 301 to 258 K the fluorescence intensity decreases which is a result of the increased complexation constant. As the concentration ratio of H_2PF and ZnPD was chosen to be ≈0.9 in this experiment, even when all H_2PF molecules will be bound to dimers non-bound ZnPD will still exist, being responsible for the remaining fluorescence. This fluorescence increases with further lowering of temperature accompanied by a slight hypsochromic shift of the pure electronic transition Q(0,0)-band. These effects are well-known for monomeric porphyrins [19] and their chemical dimers [20,21]. Even in glassy matrices of methylcyclohexane the H_2PF fluorescence remains noticeably quenched at 77 K.

3.2. Time-resolved experiments

Time-resolved spectra of the fluorinated triad are presented in Fig. 7. The main features which can be recognized are ground state bleaching of the porphyrin Q-bands at 515, 550 and 580 nm and a broad absorption at around 680 nm. From the steady-state absorption spectra the band at 515 nm

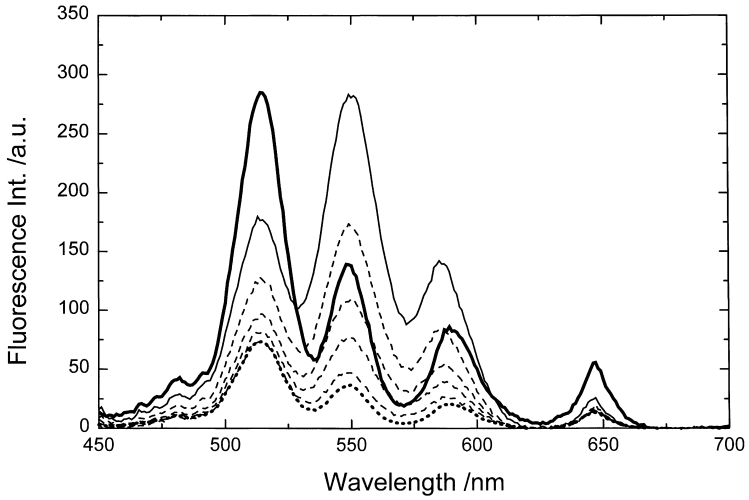

Fig. 5. Fluorescence excitation spectra of the non-fluorinated triad ($x = 0.92$, $c_{D,0} = 2.6 \times 10^{-6}$ M) in toluene plus 0 (thin solid line), 3, 6, 9, 17 vol% of acetone (thin dashed lines, intensity decreases with increasing amount of acetone). H_2P in toluene at same concentration as in triad (bold line). H_2P excitation spectrum divided by 3.83 (- - - -).

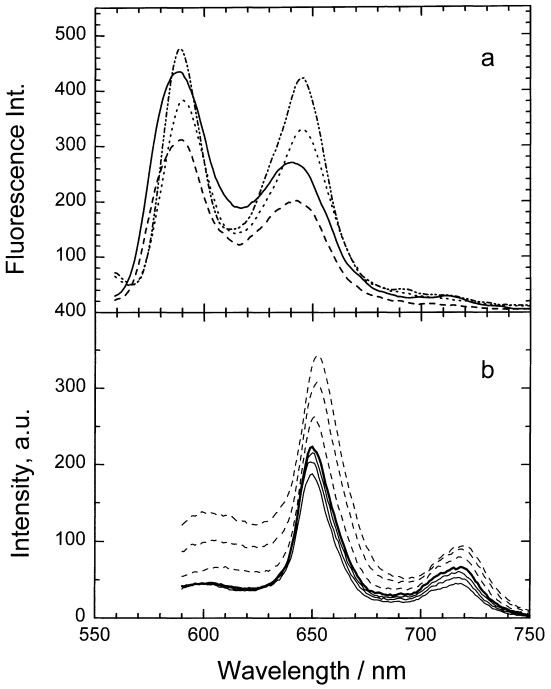

Fig. 6. (a) Fluorescence spectra ($\lambda_{ex} = 545$ nm) of fluorinated triad ($x = 0.93$, $c_{D,0} = 1.8 \times 10^{-6}$ M) at 301 K (————), 258 K (— — —), 186 K (· · · · · · ·) and 164 K (—·—·—·—). (b) Fluorescence spectra of non-fluorinated triad in toluene plus 7 vol% of acetone at different temperatures (333 K (top spectrum), 318, 293, 278 K (bold line), 263, 243, 221 K (bottom spectrum)). Intensity decreases steadily as temperature is reduced. Dashed lines are used for temperatures, where an increase of ZnPD fluorescence indicates aggregate decomposition.

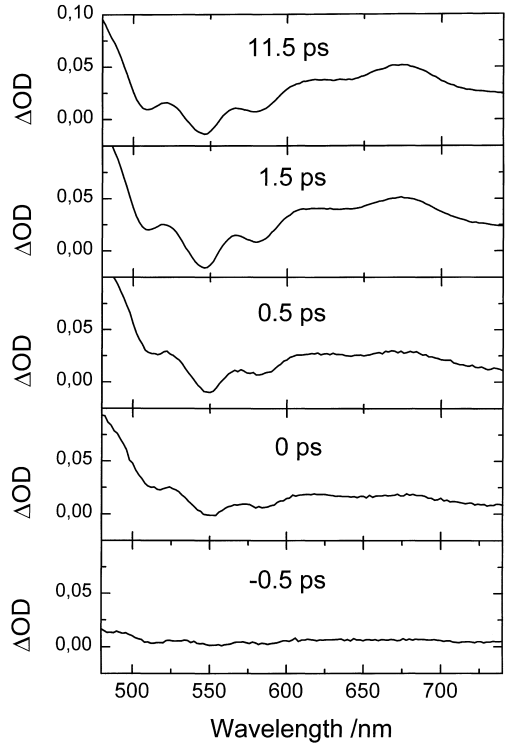

Fig. 7. Time-resolved transient absorption spectra of the fluorinated triad in toluene at 293 K at various delay times with respect to the exciting pump pulse at 400 nm.

can be assigned to the free base absorption while those at 550 and 580 nm are mainly determined by ZnPD. Absorption at 680 nm is usually ascribed to the zinc porphyrin cation [22]. The transients of the absorption at 510 and 680 nm are shown in Fig. 8. At 510 nm the OD decreases after an immediate rise at time zero. The decay was fitted with time constant 0.7 (±0.1) ps. At 680 nm an immediate rise of the OD (corresponding to the system response time) followed by a very small additional slower increase is observed. This latter part – due to its small magnitude – does not allow for an accurate determination of the risetime. Nevertheless it is in accord with the time constant of 0.7 ps found for the

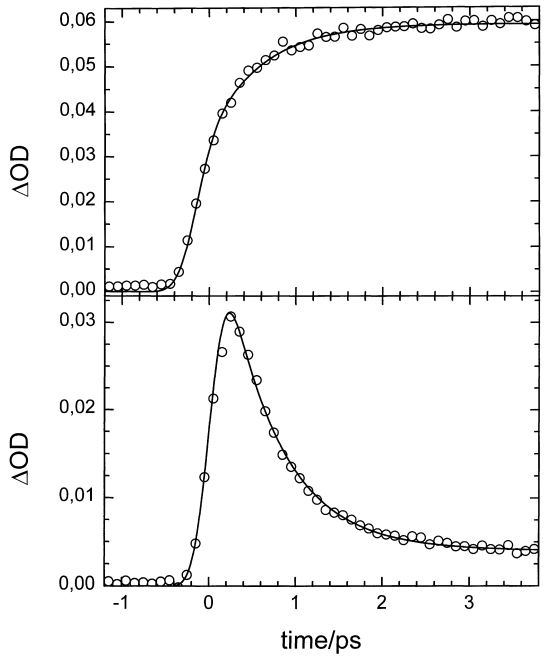

Fig. 8. Time evolution of the transient absorbance for the fluorinated triad in toluene at 293 K formed by the excitation at 555 nm and measured at 680 nm (top) and 510 nm (bottom).

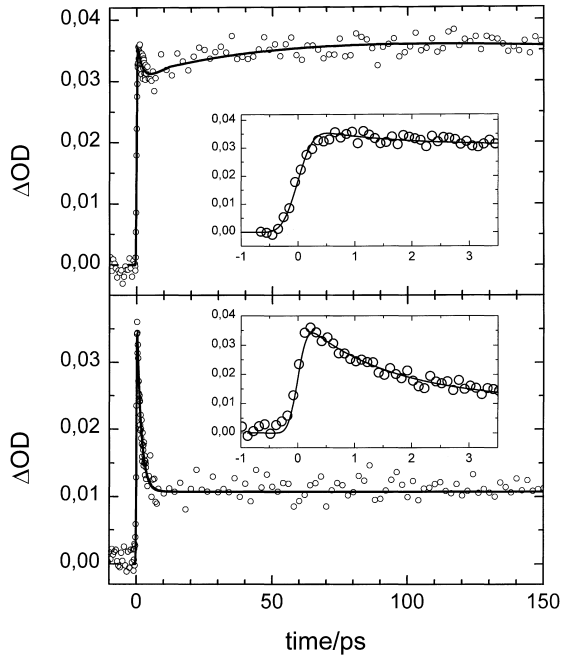

Fig. 9. Time evolution of the transient absorbance for the non-fluorinated triad pumped at 555 nm and probed at 680 nm (top) and 510 nm (bottom).

510 nm decay. A similar transient (data not shown) could be found at 890 nm where H_2PF^- is expected to absorb [23].

The time-resolved spectra of the non-fluorinated triad are quite similar to those presented for the fluorinated triad in Fig. 8. Nevertheless differences are observed in the dynamics taken at certain wavelengths (Fig. 9). The increase of H_2P ground state bleaching at 510 nm is slower as compared to the fluorinated triad: 1.6 ps versus 0.7 ps. The dynamics at 680 nm are quite complex exhibiting an immediate rise which is followed by a decay with 1.7 ps and a slower rise of 60 ps. An absorption signal at 890 nm (as for the fluorinated triad) could be found for the non-fluorinated triad in toluene plus 7 vol% of acetone but was hardly detectable in pure toluene.

As on the time scale accessible to our delay line almost no further changes in ΔOD after a few ps could be observed, one longer delay time (≈4.5 ns) was realized by introducing an additional fixed path length in the probe beam by two mirrors. The spectra taken this way (Fig. 10) at long delay may be attributed to H_2P ground state bleaching as well as to an additional broad absorption from both the first locally excited S_1- and T_1 states of H_2P [24,25].

In case of the non-fluorinated triad the fluorescence lifetimes of the free-base moiety were determined by time correlated single photon counting measurements, exciting the ZnPD moiety at 545 nm and detecting the free base fluorescence in the range 700 to 730 nm. As ZnPD fluorescence is not completely zero in the detected wavelength range (and as suppression of shorter wavelength is not complete with the interference filter used) the fluorescence transients are biexponential. The shorter lifetime has a value of 1.5 ns (changing little with acetone concentration) which is typical of ZnPD. It can be clearly attributed to fluorescence from ZnPD not bound in complexes. The longer lifetime is found to shorten slightly from 7.7 ns is pure toluene to 6.7 ns is toluene +13 vol% of acetone. The value in pure toluene is close to that measured for pure H_2P under the same conditions (9.5 ns).

4. Discussion

The titration experiments clearly demonstrate that aggregates are formed from ZnPD and H_2P or H_2PF in toluene solution like we have already shown for the non-fluorinated case in methylcyclohexane solution [14]. The complexation constant of the fluorinated triad is somewhat smaller (6×10^6) as compared to the complexation constant of the non-flourinated triad (2×10^7). Nevertheless at $K_C = 6 \times 10^{-6}\,M^{-1}$ and total concentration of dimer and extra ligand of 2×10^{-6} M this leads to 75% of molecules bound in complexes. Upon increasing the concentration to 1×10^{-5} M (as it was usual for the pump-probe experiments) this percentage is increased to 88%, i.e. the majority of molecules in our experiments performed at molar ratios of the extra ligand and ZnPD (x) = 0.9. . . 1.0 are bound in complexes. From the two coordination points between pyridyl-substituents at the free base and the zinc-ions of the dimer a structure of the aggregate like it is presented in Fig. 11 can be expected. (This structure has been calculated with the HyperChem software package (release 4, semiempirical methods AM1 and PM3) without taking solvent effects into account.)

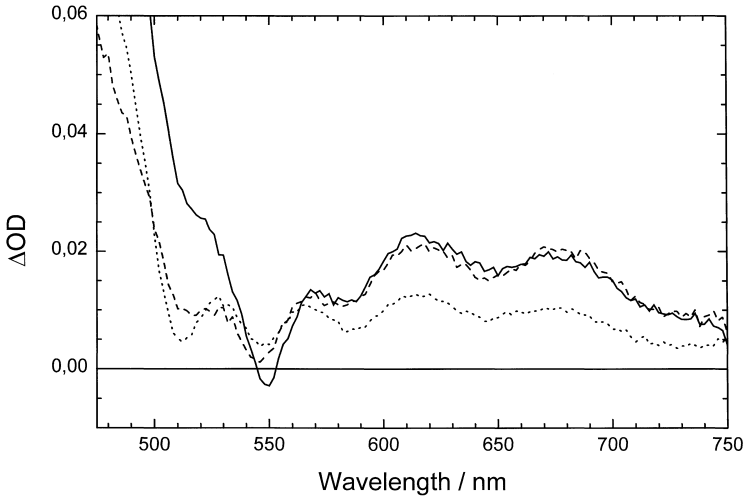

Fig. 10. Time-resolved transient absorption spectra of the non-fluorinated triad at delay times of 0.5 ps, 6.0 ps and 4.5 ns (λ_{pump} = 400 nm).

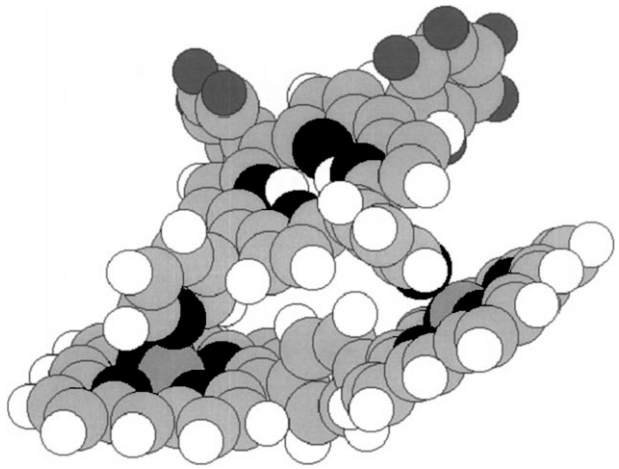

Fig. 11. Structure of the fluorinated triad calculated with the HyperChem software package in vacuum.

The striking difference between the fluorinated and non-fluorinated triad is the pronounced quenching of the free base fluorescence in the former (Fig. 2). Obviously there is an additional decay channel for the excited state of the free base in the fluorinated triad. In principal three different possibilities may be responsible for this additional depopulation process: (i) intersystem crossing to the triplet state, (ii) non-radiative decay to the ground state and (iii) formation of a charge separated state $ZnPD^{+}$ H_2PF^{-}. As there is no reason why processes (i) and (ii) should be so much increased as compared to the non-fluorinated free base we argue in favor of explanation (iii) and will discuss in the following what results further support this conclusion.

First of all we will have a look at the redox-potentials of the porphyrins under study, which determine the energetic feasibility of an electron transfer process. The free enthalpies of the charge separated state may be written as $G = E_D^{ox} - E_A^{red} + \Delta G(\varepsilon)$ [26], where E_D^{ox} is the oxidation potential of the donor, E_A^{red} the reduction potential of the acceptor and $\Delta G(\epsilon)$ accounts for the differences in dielectric constants between the solvent in which the redox potentials were measured and the solvent in which G shall be calculated as well as for coulombic interaction of the cation and anion. Although the existing expressions for calculating $\Delta G(\epsilon)$ [27] turned out to be rather questionable [28] we will use them in lack of more accurate information, being aware that the numbers calculated will give a rather rough estimation. In any case the tendencies of change in G when comparing the fluorinated and non-fluorinated triad should be reproduced correctly. In polar solvents the oxidation potential E_D^{ox} of ZnOEP is +0.63 eV (butyronitrile versus SCE) [29], the reduction potential E_A^{red} of H_2TPP is −1.08 eV (DMF versus SCE) [30] and the reduction potential of a free base porphyrin with three fluorinated phenylgroups is −0.85 (benzonitrile versus SCE) [31]. With [26,27]

$$\Delta G = E_D^{ox} - E_A^{red} + \frac{e^2}{4\pi\varepsilon_0}\left[\left(\frac{1}{2r_D} + \frac{1}{2r_A} - \frac{1}{r_{DA}}\right)\frac{1}{\varepsilon} - \left(\frac{1}{2r_D}\frac{1}{\varepsilon'_D} + \frac{1}{2r_A}\frac{1}{\varepsilon'_A}\right)\right];$$

$r_D = r_A = 5.5$ Å and $r_{DA} = 8.8$ Å from the calculated structure; ε (butyronitrile) = 24.8, ε (benzonitrile) = 25.2, ε (DMF) = 36.7; ε (toluene) = 2.38 we obtain $\Delta G_{nf} = 2.03$ eV for the non-fluorinated triad and $\Delta G_f = 1.79$ eV for the fluorinated triad. Taking into account that pyridyl substituents increase the reduction potential of free base porphyrins ($E_A^{red}(H_2(mPyr)_4P) = -0.95$ eV in DMF versus SCE [32]) the values of ΔG will be lowered to $\Delta G_{nf} = 1.90$ eV and $\Delta G_f = 1.66$ eV. (In principle the extra-ligand to ZnOEP will change its oxidation potential [33]. Nevertheless the oxidation potential taken from [29] was measured with tetrabutylammonium perchlorate as supporting electrolyte. It has been shown that this supporting electrolyte coordinates to ZnTPP thus causing a similar effect on the oxidation potential like a pyridin extra-ligand [33]. We therefore use

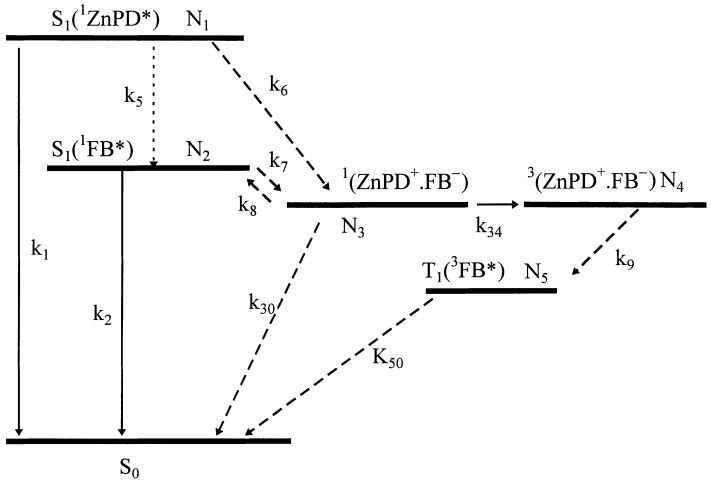

Fig. 12. Schematic energy level diagram for low-lying locally excited singlet states of ZnPD $\{S_1(^1ZnPD^*)$, population $N_1\}$, H_2PF or H_2P $\{S_1(^1FB^*)$, population $N_2\}$, locally excited triplet state of H_2PF or H_2P $\{T_1(^3FB^*)$, population $N_5\}$ state, charge-transfer singlet state $\{^1(ZnPD^+...FB^-)$, population $N_3\}$ and charge-transfer triplet state $\{^3(ZnPD^+...FB^-)$, population $N_4\}$. Indicated are rate constants of the following pathways: k_1, radiative and non-radiative decay of ZnPD*; k_2, radiative and non-radiative decay of H_2P; (intersystem crossing from the singlet to the triplet state $S_1 \rightarrow T_1$ is not presented); k_7, hole transfer from the extra-ligand locally excited singlet state to ZnPD forming the singlet radical ion pair state; k_8, charge recombination from the singlet radical ion pair state to the extra-ligand locally excited singlet state (thermally activated for non-fluorinated extra-ligand); k_{34}, spin rephasing between the singlet and triplet radical ion pairs; k_{30}, charge recombination from the singlet radical ion pair to the ground state; k_{50}, non-radiative intersystem crossing to the ground state, $T_1 \rightarrow S_0$; k_9, charge recombination from the triplet radical ion pair to the locally excited triplet state of an extra-ligand.

the oxidation potential for ZnOEP from [29] as being very close to that of pyridinated ZnOEP). The excited state of the free base is at 1.91 eV (in both cases) i.e. the charge transfer state is approximately isoenergetic in case of the non-fluorinated triad while it is 0.25 eV lower in case of the fluorinated triad. Therefore the difference in fluorescence quenching for extra-ligands in the two triads can be explained by the energetic feasibility of a charge transfer to a considerably lower (≈10 kT) lying state in case of the fluorinated triad. In the non-fluorinated triad, on the other hand, an equilibrium between the ZnPD-H_2P^* excited state and the $ZnPD^+$-H_2P^- charge separated state will be responsible for the partial quenching of free base fluorescence while not changing fluorescence lifetime a lot. We will discuss this topic in more detail later on.

Before we do so we would like to point out, that the energy level scheme as outlined above and shown in Fig. 12 is also in accord with the temperature dependence of the non-fluorinated triad fluorescence spectra (Fig. 6). As already mentioned in Section 3 the constant intensity of the ZnPD fluorescence band at 600 nm in the temperature range below 278 K indicates that aggregation is complete and any changes in intensity are not due to triad composition or decomposition. The intensity of the H_2P fluorescence band at 720 nm was therefore fitted to a Boltzman distribution function (const. + $1/(1 + \exp\{\Delta E/kT\})$) only in this temperature range (Fig. 13). It yields $\Delta E = 0.05$ eV in case of toluene + 7 vol% of acetone, while almost no activation energy is found in pure toluene. The latter agrees well with the above finding of $\Delta G \approx E(\text{ZnPD-}H_2P^*) = 1.91$ eV. Increasing the solvent polarity will decrease ΔG (and the activation enthalpy $\Delta G^{\#}$) thus leading to the activation energy observed.

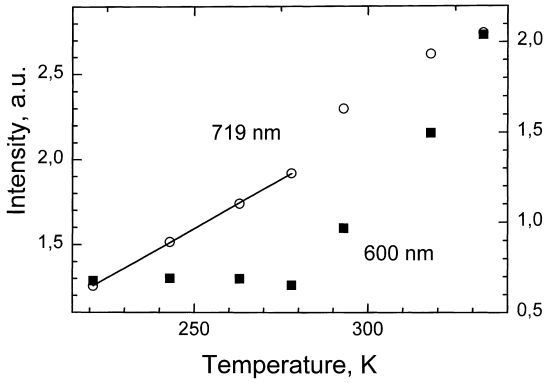

Fig. 13. Intensity of the H_2P fluorescence band at 719 nm and the ZnPD fluorescence band at 600 nm, as taken from the spectra in Fig. 6(b). (————) is a fit to a two level Boltzman distribution as described in the text.

To estimate this effect the dielectric constant of the mixture was calculated assuming that the Onsager function of the mixture is a sum of the Onsager functions of the individual components [34]. For 7 vol% of acetone a change of ε from 2.38 to 2.64 is determined in this way. Calculating ΔG with this ε leads to a reduction of ΔG by 0.04 eV which corresponds (surprisingly well) to the measured activation energy of 0.05 eV.

The dependence of the steady-state fluorescence spectra of the non-fluorinated triad on the dielectric constant of the solvent indicate that both energy and charge transfer processes may play a role in the dynamics of this aggregate. Quite obviously there is energy transfer from ZnPD to the free base in this case which leads to stimulated fluorescence (Figs. 4 and 5). At present we cannot decide whether this is

via direct energy transfer (k_5 in Fig. 12) or is due to combined charge transfer processes ($k_6 + k_8$ in Fig. 12). Nevertheless free base fluorescence is quenched by increasing the polarity of the solvent (addition of acetone), which may hint to an electron transfer process involved even in this case. The excitation spectra in Fig. 5 show that this quenching of free base fluorescence is not due to faster depopulation of the excited state of the free base but due to a reduction in the amount of energy transferred from ZnPD. The excitation band at 646 nm, where only free base is excited does not change upon addition of acetone, while the bands at 549 and 585 nm, where ZnPD is excited, are reduced, so that finally an excitation spectrum remains, which is almost identical to the one of pure free base.

Analyzing the time-resolved spectra it is necessary to keep in mind that pumping at 555 nm leads mainly to excitation of the zinc porphyrin moiety (ε (ZnPD) $\approx 18 \times \varepsilon$ (H_2PF), ε (ZnPD) $\approx 4 \times \varepsilon$ (H_2P)). The immediate rise of the OD is attributed to excited state absorption of ZnPD [24]. Further additional growth at 680 nm may be ascribed to absorption of $ZnOEP^+$ [35,36]. Nevertheless excited state absorption of singlet and triplet states of all moieties involved has to be taken into account at this wavelength too. At 510 nm again the excited state absorption of ZnPD yields the immediate increase of the OD, while ground state bleaching of H_2PF or H_2P is responsible for the decay following this increase. For the fluorinated triad we find almost no change of the bleaching signal of ZnPD (at 550 and 580 nm) which clearly indicates that ZnPD* does not return to its ground state during this time. Therefore it does not transfer its energy to H_2PF and the increased bleaching of H_2PF at 510 nm is attributed to production of the H_2PF radical anion. The dynamics at 510 nm (Fig. 8) indicate a time constant of 0.7 ± 0.2 ps for this transfer process. No pronounced spectral changes are observed at 680 nm where $ZnOEP^+$ is expected to absorb [36]. Only a slight increase can be observed on the kinetic traces in Fig. 8. Nevetherless this increase agrees well with the 0.7 ps determined for the 510 nm dynamics. The fact that there is no pronounced $ZnPD^+$ spectral feature at 680 nm agrees well with experiments performed on a covalentely linked system with the electron acceptor pyromellitimide (PIm) attached to ZnPD. In this system we clearly observed the PIm^- spectral feature at 720 nm [37] (as it is described by many authors e.g. in [38]) while the absorption spectrum is rather flat at 680 nm. The dynamics observed at both wavelength coincide within experimental error. The dynamics at 890 nm where H_2PF^- is expected to absorb [23,39] support the production of a charge separated state. They are quite similar to those at 680 nm i.e. an immediate rise followed by a fast small further increase. Summarizing we argue that an extremely fast electron transfer takes place on a time scale of 0.7 ps. As there is no increase of free-base fluorescence in the steady-state spectra upon lowering of temperature (Fig. 6) we conclude that this transfer is still effective at 164 K. This electron transfer process has to be compared to the one observed in a similar system, where a zinc-porphyrin is covalently linked to a free base porphyrin with three pentafluorophenyl substituents [23]. These authors report an electron transfer from the excited zinc-porphyrin or the excited free-base porphyrin with $(71\,\text{ps})^{-1}$ and $(222\,\text{ps})^{-1}$ respectively, while the decay of the charge separated state is even faster $(8\,\text{ps})^{-1}$. Thus the system presented here shows a much shorter charge separation time. We attribute this to much increased overlap of donor and acceptor electronic wavefunctions as in the case ZnPD and H_2PF are face to face with a short distance between the porphyrin planes of approximately 3.5 Å while in the covalently linked system of [23] they are edge-to-edge at large distance of approximately 14 Å. The measured transient time resembles more those observed in bacterial photosynthesis of a few 100 fs to a few ps [40,41]. These natural systems too do show efficient charge transfer at low temperatures [42] while only few model systems with this property have been described [43]. We ascribe the high efficiency of charge transfer at low temperature to stabilization of the ZnP^+ radical cation by the pyridyl ligands.

The absorption transients of the non-fluorinated triad do show slower dynamics. The H_2P bleaching 515 nm shows that H_2P^* or H_2P^+ are formed with time constant of 1.6 ps. From the steady-state spectra it is obvious that sensitization via ZnPD absorption is involved. The complex dynamics at 680 nm are attributed to the superposition of the absorption of all of the following states: ZnPD*, H_2P^* and $ZnPD^+H_2P^-$. To explain this qualitatively we calculated the dynamics for the energy level scheme as depicted in Fig. 12. The following rates were used: $k_1 = 8.33 \times 10^8$ (from the ZnPD fluorescence lifetime of 1.2 ns), $k_2 = 1.05 \times 10^8$ (from the H_2P fluorescence lifetime of 9.5 ns), $k_3 = (k_{30} + k_{34}) = 2.00 \times 10^8$ (from the signal decrease found at long delay of 4.5 ns which yields an estimated decay time of 5 ns), $k_5 = 5.0 \times 10^{11}$, $k_6 = 1.25 \times 10^{11}$ ($(k_5 + k_6)^{-1} = 1.6$ ps from the kinetics at 515 nm, the ratio between k_5 and k_6 chosen arbitrarily), $k_7 = 1.67 \times 10^{10}$ (from the 'slow' 60 ps rise of the 680 nm transient) and k_8 was calculated as $k_7 \exp(-\Delta E/kT)$ where ΔE is the energy difference between the excited state of H_2P and the charge separated state. For $\Delta E = 0$ this leads to a simulated signal as it is depicted in Fig. 14. This simulated signal qualitatively reproduces the principle from the measured data in Fig. 9. As it was impossible to access all of the rates involved individually it cannot be excluded that other combinations of rates (specially different ratio k_5/k_6) would lead to a similar result. This calculation does explain the behavior of the H_2P fluorescence quantum yield and lifetime as well. Changing ΔE from 0 to 0.05 eV leads to a change in the population lifetime (i.e. fluorescence lifetime) of H_2P^* from 6.6 to 5.3 ns while the integrated population number (which is proportional to the quantum yield) changes from 3.3 to 0.7 arb. units. This reproduces the observation of little change in lifetime while pronounced changes in fluorescence intensity occur.

Both in the fluorinated and non-fluorinated triad almost no decay is observed in the transients. This leads to the

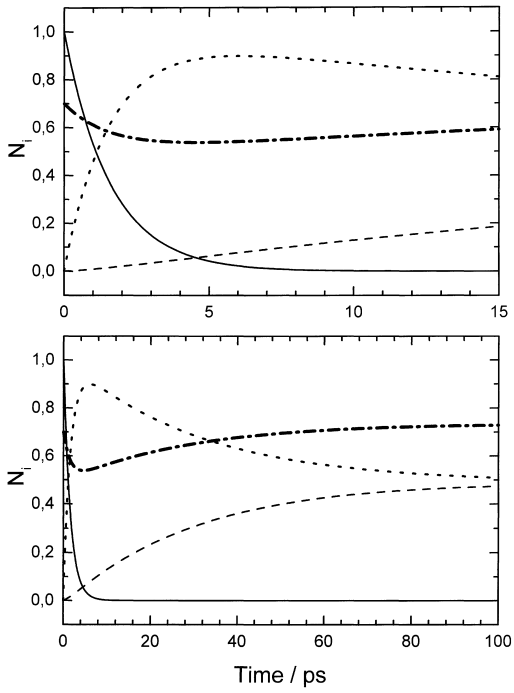

Fig. 14. Simulated time dependence of the population of the levels as shown in Fig. 12: $N_1(t)$ (————), $N_2(t)$(— — —) and $N_3(t)$ (------) and $0.8 \times N_1(t) + 0.5 \times N_2(t) + 1.0 \times N_3(t)$ (· – · – · –). For details see text.

conclusion, that on the timescale accessible to our setup (≈670 ps) there is only minor decay to the ground state. Our comparative studies using a nanosecond flashphotolysis experimental setup have shown that in toluene or MCH (room temperatures, non-degassed solutions) the amplitudes of transient triplet–triplet absorption spectra in the region of 440–470 nm for H_2PF in the fluorinated triad are almost the same as those obtained for H_2P in the non-fluorinated triad under the same experimental conditions ($\lambda_{ex} = 532$ nm, $\Delta t_{1/2} = 20$ ns). Additionally, the lifetimes of these transients were found to be almost the same for these extra-ligands in their triads ($\tau_T = 335$ ns for H_2PF and $\tau_T = 355$ ns for H_2P). The same values of τ_T were obtained for individual extra-ligands which are typical of porphyrin free bases in liquid solutions at room temperature in the presence of oxygen [44,45]. Finally, it can be seen from Fig. 10 that the transient absorption spectrum of the non-fluorinated triad at approximately 4.5 ns delay time differs principally from that detected at short delay times. The bleaching bands of this spectrum are rather 'free-base like' while at the short time delays they are 'triad-like' i.e. a superposition of the H_2P and ZnPD absorption bands. The spectrum at late times corresponds better to known T–T spectra for porphyrins free bases [24,25]. On the base of all these facts it is reasonable to assume that the population of the locally excited T_1-state of fluorinated extra-ligand in the triad $T_1(^3FB^*)$ takes place from the upper-lying triplet radical ion pair state $^3(ZnPD^+ \ldots FB^-)$, or directly from the singlet radical ion pair state $^1(ZnPD^+ \ldots FB^-)$ taking into account the fact that the spin-exchange energy is negligible and the spin rephasing between the singlet and triplet radical ion pairs is rather effective [46]. Further it is clear from photophysical parameters (the rate constant of the non-radiative intersystem crossing $S_1 \rightarrow T_1$ of $5.0 \times 10^7\ s^{-1}$ and the radiative rate constant of $5.0 \times 10^6\ s^{-1}$ known for porphyrin free bases [21,44,45] and estimated values of the electron transfer rate constants k_6, $k_7 > 10^{10}\ s^{-1}$), that direct population of the T_1 state of the fluorinated extra-ligand via intersystem crossing $S_1(^1FB^*) \rightarrow T_1(^3FB^*)$ is probably low in the triad.

5. Conclusions

Two different triadic aggregates formed from the zinc porphyrin dimer ZnPD and the free base H_2P or H_2PF have been investigated. Steady-state and time-resolved optical spectroscopic data indicate fast electron and energy transfer from the zinc porphyrin to the free base porphyrin. In case of the triad formed with the fluorinated free base porphyrin H_2PF the charge transfer state is considerably lower in energy than the excited states of both ZnPD and H_2PF and efficient charge transfer faster than 1 ps occurs. This charge transfer cannot be slowed down remarkably by cooling down to temperatures of 164 K. In the non-fluorinated triad the competition of charge transfer and energy transfer between ZnPD and H_2P cause rather complex dynamics. They are interpreted as being due to the equilibriation process between the H_2P excited state and a close lying charge separated state. In both triads the decay to the ground state is via the free base triplet state and occurs on a time scale of some ns.

Acknowledgements

This research was supported by the Deutsche Forschungsgemeinschaft (SCHR 231/14-2) and the Volkswagenstiftung (No. I/68 941).

References

[1] M.R. Wasielewski, Chem. Rev. 92 (1992) 435.
[2] J.L. Sessler, V.L. Capuano, A. Harriman, J. Am. Chem. Soc. 115 (1993) 4618.
[3] S.-C. Hung, A.N. Macpherson, S. Lin, P.A. Liddell, G.R. Seely, A.L. Moore, T.A. Moore, D. Gust, J. Am. Chem. Soc. 117 (1995) 1657.
[4] A. Osuka, H. Yamada, S. Shinoda, K. Nozaki, T. Ohno, Chem. Phys. Lett. 238 (1995) 37.
[5] V.S.-Y. Lin, S.G. DiMagno, M.J. Therien, Science 264 (1994) 1105.
[6] A. Osuka, S. Marumo, N. Mataga, S. Taniguchi, T. Okada, I. Yamazaki, Y. Nishimura, T. Ohno, K. Nozaki, J. Am. Chem. Soc. 118 (1996) 155.
[7] M.P. Debreczeny, W.A. Svec, M.R. Wasielewski, Science 274 (1996) 584.
[8] Y. Aoyama, M. Asakawa, Y. Matsui, H. Ogoshi, J. Am. Chem. Soc. 113 (1991) 6233.
[9] J.L. Sessler, B. Wang, A. Harriman, J. Am. Chem. Soc. 117 (1995) 704.

[10] I. Salabert, T.-H. Tran-Thi, H. Ali, J. van-Lier, D. Houde, E. Keszei, Chem. Phys. Lett. 223 (1994) 313.
[11] M. Ikonen, D. Guez, V. Marvaud, D. Markovitsi, Chem. Phys. Lett. 231 (1994) 93.
[12] H. Tamiaki, T. Miyatake, R. Tanikaga, A.R. Holzwarth, K. Schaffner, Angew. Chem. Int. Ed. Engl. 35 (1997) 772.
[13] J.A.I. Oksanen, E.I. Zenkevich, V.N. Knyukshto, S. Pakalnis, P.H. Hynninen, J.E.I. Korrpi-Tommola, Biochim. Biophys. Acta 1321 (1997) 165.
[14] A.V. Chernook, A.M. Shulga, E.I. Zenkevich, U. Rempel, C. von Borczyskowski, J. Phys. Chem. 100 (1996) 1918.
[15] A.V. Chernook, U. Rempel, C. von Borczyskowski, A.M. Shulga, E.I. Zenkevich, Chem. Phys. Lett. 254 (1996) 229.
[16] R.G. Little, J.A. Anton, P.A. Loach, J.A. Ibers, J. Heterocycl. Chem. 12 (1975) 343.
[17] G.H. Barnet, M.F. Hudson, K.M. Smith, J. Chem. Soc. Perkin Trans. 1 1975 (1975) 1401.
[18] J.R. Miller, G.D. Dorough, J. Am. Chem. Soc. 74 (1952) 3977.
[19] K.N. Solov'ev, V.N. Knyukshto, M.P. Tzvirko, Optics Spectroscopy 41 (1976) 964.
[20] U. Rempel, B. von Maltzan, C. von Borczyskowski, Z. Phys. Chem. 170 (1991) 107.
[21] E.I. Zenkevich, A.M. Shulga, A.V. Chernook, G.P. Gurinovich, Chem. Phys. Lett. 109 (1984) 306.
[22] A. Osuka, S. Nakajima, K. Maruyama, N. Mataga, T. Asahi, Chem. Lett. 1991 (1991) 1003.
[23] D. Gust, T.A. Moore, A.L. Moore, L. Leggett, S. Lin, J.M. DeGraziano, R.M. Hermant, D. Nicodem, P. Craig, G.R. Seely, R.A. Nieman, J. Phys. Chem. 97 (1993) 7926.
[24] J. Rodriguez, C. Kirmaier, D. Holton, J. Am. Chem. Soc. 111 (1989) 6500.
[25] B.M. Dzhagarov, E.I. Sagun, G.P. Gurinovich, J. Appl. Spectr. 15 (1971) 476.
[26] G.J. Kavarnos, N.J. Turro, Chem. Rev. 86 (1986) 401.
[27] A. Weller, Zeitschrift für Phys. Chem. Neue Folge 133 (1982) 93.
[28] J.A. Schmidt, J.-Y. Liu, J.R. Bolton, M.D. Archer, V.P.Y. Gadzekpo, J. Chem. Soc., Faraday Trans. 85 (1989) 1027.
[29] J.-H. Fuhrhop, K.M. Kadish, D.G. Davis, J. Am. Chem. Soc. 95 (1973) 5140.
[30] D. Dolphin (Ed.), The Porphyrins, vol. V, Academic Press, New York, 1978
[31] D. Gust, T.A. Moore, A.L. Moore, F. Gao, D. Luttrull, J.M. DeGraziano, X.C. Ma, L.R. Makings, S.-J. Lee, T.T. Trier, E. Bittersmann, G.R. Seely, S. Woodward, R.V. Bensasson, M. Rougée, F.C. De Schryver, M. Van dr Auweraer, J. Am. Chem. Soc. 113 (1991) 3638.
[32] P. Worthington, P. Hambright, R. Williams et. al., J. Inorg. Biochem. 12 (1980) 281.
[33] D. Gust, T.A. Moore, A.L. Moore, H.K. Kang, J.M. DeGraziano, P.A. Liddell, G.R. Seely, J. Phys. Chem. 97 (1993) 13637.
[34] P. Suppan, J. Chem. Soc. Faraday Trans. I 83 (1987) 495.
[35] J.H. Fuhrhop, D. Mauzerall, J. Am. Chem. Soc. 91 (1969) 4174.
[36] D.G. Johnson, M.P. Niemczyk, D.W. Minsek, G.P. Wiederrecht, W.A. Svec, G.L. Gaines III, M.R. Wasielewski, J. Am. Chem. Soc. 115 (1993) 5692.
[37] E.I. Zenkevich, S.M. Bachilo, A.M. Shulga, U. Rempel, A. Willert, C. von Borczyskowski, Mol. Cryst. Liq. Cryst. 324 (1998) 169.
[38] A. Osuka, S. Marumo, K. Maruyama, N. Mataga, M. Ohkohchi, S. Taniguchi, T. Okada, I. Yamazaki, Y. Nishimura, Chem. Phys. Lett. 225 (1994) 140.
[39] G. Peychal-Heiling, G.S. Wilson, Anal. Chem. 43 (1971) 550.
[40] S. Schmidt, F. Arlt, P. Hamm, H. Huber, T. Nägele, J. Wachtveitl, M. Meyer, H. Scheer, W. Zinth, Chem. Phys. Lett. 223 (1994) 116.
[41] M. Bixon, J. Jortner, M.E. Michel-Beyerle, Chem. Phys. 197 (1995) 389.
[42] G.R. Fleming, J.-L. Martin, J. Breton, Nature 333 (1988) 190.
[43] M.R. Wasielewski, D.J. Johnson, W.A. Swec, K.M. Kersey, D.W. Minsek, J. Am. Chem. Soc. 110 (1988) 7219.
[44] V.A. Ganzha, G.P. Gurinovich, B.M. Dzhagarov, G.D. Egorova, E.I. Sagun, A.M. Shulga, Zhurnal Prikladnoi Spektr. 50 (1989) 618.
[45] E. Zenkevich, E. Sagun, V. Knyukshto, A. Shulga, A. Mironov, O. Efremova, R. Bonnett, S. Pinda Songca, M. Kassem, J. Photochem. Photobiol. B: Biol. 33 (1996) 171.
[46] D.D. Fraser, J.R. Bolton, J. Phys. Chem. 98 (1994) 1626.